**Proceedings of the ASME 2011 Pacific Rim Technical Conference & Exposition on Packaging and Integration of Electronic and Photonic Systems**
**InterPACK2011**
**July 6-8, 2011, Portland, Oregon, USA**

# IPACK2011-52191

# EXERGY ANALYSIS AND ENTROPY GENERATION MINIMIZATION OF THERMOELECTRIC WASTE HEAT RECOVERY FOR ELECTRONICS

**Kazuaki Yazawa**
University of California Santa Cruz
Santa Cruz, CA, U.S.A.

**Ali Shakouri**
University of California Santa Cruz
Santa Cruz, CA, U.S.A.

## ABSTRACT

Energy recovery from waste heat is attracting more and more attention. All electronic systems consume electricity but only a fraction of it is used for information processing and for human interfaces, such as displays. Lots of energy is dissipated as heat. There are some discussions on waste heat recovery from the electronic systems such as laptop computers. However the efficiency of energy conversion for such utilization is not very attractive due to the maximum allowable temperature of the heat source devices. This leads to very low limits of Carnot efficiency. In contrast to thermodynamic heat engines, Brayton cycle, free piston Stirling engines, etc., authors previously reported that thermoelectric (TE) can be a cost-effective device if the TE and the heat sink are co-optimized, and if some parasitic effects could be reduced. Since the heat already exists and it is free, the additional cost and energy payback time are the key measures to evaluate the value of the energy recovery system. In this report, we will start with the optimum model of the TE power generation system. Then, theoretical maximum output, cost impact and energy payback are evaluated in the examples of electronics system. Entropy Generation Minimization (EGM) is a method already familiar in thermal management of electronics. The optimum thermoelectric waste heat recovery design is compared with the EGM approach. Exergy analysis evaluates the useful energy flow in the optimum TE system. This comprehensive analysis is used to predict the potential future impact of the TE material development, as the dimensionless figure-of-merit (ZT) is improved.

## INTRODUCTION

Waste heat recovery from electronic systems has been receiving attention but not reported very much relative to energy harvesters such as Piezo electric from vibration [1], powering from human hand winding motion [2], and embedded film solar cells [3]. A few studies on waste heat exist in the literature, such as the waste recovery from a laptop [4]. The reason might be disappointment with insufficient power output due to the small temperature differences available across heat engines, even with high energy conversion efficiency. This is limited by Eq. (1) in a system including thermal dissipation with an ideal heat engine, as found by Curzon and Ahlborn [5]. This is smaller than Carnot efficiency.

$$\eta_{CA} = 1 - \sqrt{\frac{T_a}{T_s}} \tag{1}$$

where $T_s$ is the source temperature and $T_a$ is the ambient temperature. This is also true for the thermoelectric if extremely large ZT is assumed but only for the symmetric external heat dissipation [6].

There are technologies developed as heat engines like the Brayton cycle, free piston Stirling engines, etc. These are actually used in various power plants. The system efficiencies were discussed by Esposito [7]. All these technologies fall under the same energy conversion principle. Authors have looked into thermoelectric direct energy conversion since the optimum design of the thermoelectric was found to be cost-effective [8] if some


Copyright © 2011 by ASME

parasitic effects are reduced, such as contact resistances, heat leak (cross talk) and CTE mismatch. As thermoelements (legs) are designed to become smaller and thinner at the same time, the thermoelectric material can be saved by nearly the square of the size. So, the trade off here is that when you make the elements smaller, you increase thermal spreading resistance.. Therefore, in creating a model, we took into account the optimum packing.. Since the waste heat is free, the energy payback was investigated in the previous report [4] for cost discussion. We then quantitatively investigated how much changed in quality of heat during the energy conversion process. There is a method called Entropy Generation Minimization (EGM) originally proposed by Bejan [9], which yields a system designed to minimize the production of energy loss. The exergy would be the metric to evaluate the quality of energy. In this report, we will use these two measures to quantify the thermoelectric waste heat recovery.

## THERMOELECTRIC POWER GENERATION

The generic thermoelectric power generation model was developed and the optimum for maximum power output was determined in the previous work as the following figure and equations.

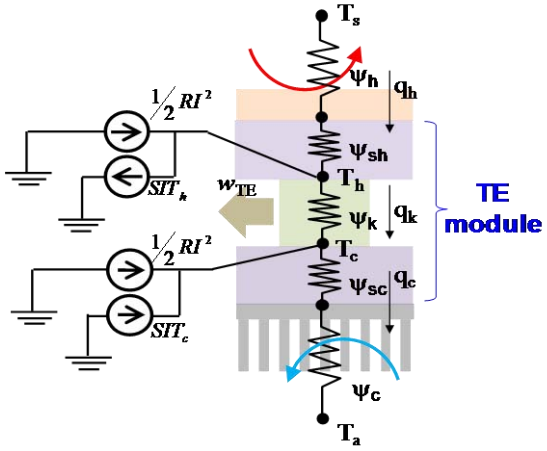


Figure 1. Equivalent thermal circuit of the TE module with heat source and heat sink

Eqs. (2) and (3) are developed from the energy balance at two nodes, $T_h$ and $T_c$, which are the temperatures at the hot side and cold side respectively of the thermoelectric element. In this model, we consider the unit cross section area for the geometrically related parameters.

$$q_h = \frac{\beta}{d}(T_h - T_c) + SIT_h - I^2R/2 \tag{2}$$

$$q_c = \frac{\beta}{d}(T_h - T_c) + SIT_c + I^2R/2 \tag{3}$$

where $\beta$ is the thermal conductivity, $d$ is the leg length, $S$ is the Seebeck coefficient, $I$ is the electrical current, and $R$ is the thermoelectric internal resistance. The current $I$ in the circuit is determined by

$$I = \frac{\sigma S}{(1+m)d}(T_h - T_c) \tag{4}$$

where $\sigma$ is electrical conductivity. $m$ is the resistance ratio of $R_L$: the load resistor with respect to $R$. The output power density $w$ is found with $T_s$ and $T_a$ substituted from $T_h$ and $T_c$.

$$w = \frac{mZ}{(1+m)^2}\frac{d\beta}{\left(d+\beta\sum\psi X\right)^2}(T_s - T_a)^2 \tag{5}$$

where $\Sigma\psi$ is the sum of the thermal resistances at the hot and cold sides. In $X$ the thermal resistance ratio is found as

$$X = \left(1+\frac{Z}{2(1+m)^2}((2m+1)T_h + T_c)\right)\frac{\psi_h}{\sum\psi} + \left(1+\frac{Z}{2(1+m)^2}(T_h + (2m+1)T_c)\right)\frac{\psi_c}{\sum\psi} \tag{6}$$

where $Z$ is the figure-of-merit of thermoelectric material known as

$$Z = \frac{\sigma S^2}{\beta} \tag{7}$$

Optimizing the thermoelectric leg length yields $d_{opt}$, and the maximum output $w_{max}$,

$$d_{opt} = \beta\sum\psi X \tag{8}$$

$$w_{\max} = \frac{mZ}{(1+m)^2}\frac{(T_s - T_a)^2}{4X\sum\psi} \tag{9}$$

Similarly, $m_{opt}$ is found.

$$m_{opt} = \sqrt{1+Z\frac{(T_h+T_c)}{2}} \tag{10}$$

As the special case $\psi_c/\psi_h$=1 (symmetric dissipation),

$$X_{opt} = \left(1+\frac{Z(T_h+T_c)}{2(1+m)}\right) = m_{opt} \tag{11}$$

Only for the symmetric dissipation, the optimum factor for the electrical resistance $m$ and that for the thermal resistance $X$ are identical.


Copyright © 2011 by ASME

## ENERGY PAYBACK

To gain some energy by the heat recovery, additional thermal resistance must be introduced by integrating a thermoelectric module in the heat flow. Increasing thermal resistance requires a smaller thermal resistance, resulting in higher pumping power to maintain the same source temperature Ts. The energy payback can be calculated by using a relation of heat transfer performance and pumping power while the heat sink is optimally designed for minimizing pump power. The net gain of the system becomes,

$$w = w_{\max} - (w_{pp\_TE} - w_{pp}) \tag{12}$$

where $w_{pp\_TE}$ is pumping power for TE integration and $w_{pp}$ is pumping power without TE integration.

Authors notice the thermal shunt approach by Solbrekken et al. [10] to avoid the direct impact on thermal resistance in the main heat path. However, limiting the thermoelectric heat flow lowers the heat flux and results in smaller power output. Since we are aiming to maximize the power output at the allowable junction temperature, this is not an ideal solution.

The minimum pumping power $w_{pp}$ is found by following formulations.

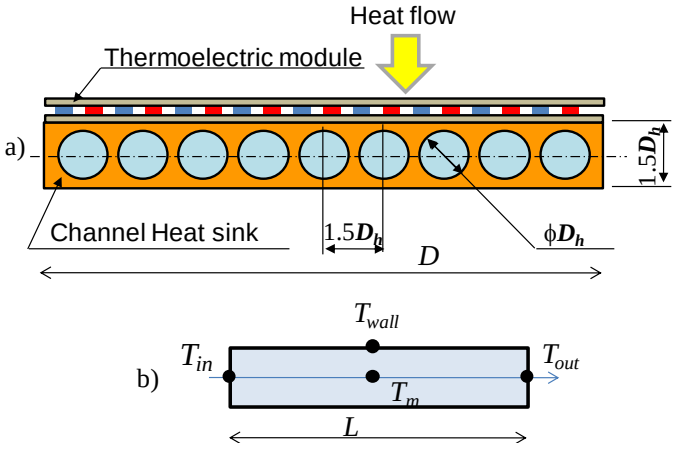


Figure 2. Universal heat sink model. a) shows the cross section perpendicular to the flow passage, and b) shows the cross section of the channel. The number of channels $N$ varies depending on the device size $A = DL$.

From Yazawa et al. [4], the thermal resistance match between the temperature sensitive mass flow and the convection yields the maximum heat transport $U_B A_B$,

$$U_B A_B = 1/\left(\frac{1}{2\rho C_p G} + \frac{1}{N U_{fin} A_{fin}}\right) \tag{13}$$

where $U_B$ is the effective heat transfer coefficient from the device area $A_B$. We look at the optimum thermal resistances match condition, described as

$$2\rho C_p G = N U_{fin} A_{fin} \tag{14}$$

Thus,

$$U_B = \frac{\rho C_p G}{DL} \tag{15}$$

The surface area $A_{fin}$ of the convective heat transfer in a single channel is

$$A_{fin} = \pi D_h L \tag{16}$$

The heat transfer coefficient of the above area is found as

$$U_{fin} = \frac{Nu\beta_f}{D_h} \tag{17}$$

where $Nu$ is the Nusselt number and was found to be a constant 4.634 for circular channels [11]. The number of channels is defined by the channel diameter $D_h$ as

$$N = \frac{2D}{3D_h} - 1 \cong \frac{2D}{3D_h} \tag{18}$$

The optimum thermal resistances match, substituting Eqs. (16) and (17) into Eq. (14),

$$G = \frac{2\pi Nu\beta_f DL}{3\rho C_p D_h} \tag{19}$$

Substituting Eq. (19) into Eq. (15),

$$D_h = \frac{2\pi Nu\beta_f}{3U_B} \tag{20}$$

The flow bulk velocity u is found as

$$u = \frac{4G}{N\pi D_h^{\,2}} \tag{21}$$

Assuming laminar flow and small contraction and expansion losses, the pressure drop across the channel is

$$\Delta P_{ch} = \frac{48\mu L}{D_h^{\,2}} u \tag{22}$$

Consolidating Eqs, (19)-(22), pumping power as a function of $U_B$ is found as


Copyright © 2011 by ASME

$$w_{pp} = G\Delta P_{ch} = \frac{972\mu DL^3}{\pi^4 \left(Nu\beta_f\right)^3 \left(\rho C_p\right)^2} U_B{}^5$$

Finally,

$$w_{pp} \cong \frac{10\mu DL^3}{\left(Nu\beta_f\right)^3 \left(\rho C_p\right)^2} U_B{}^5 \qquad (23)$$

## EXAMPLE STUDY

When applied to use in say, a laptop [4], the results could be valuable, since it addresses the question of whether the waste heat from a microprocessor can be recovered to electric power. It also addresses the matter of efficiency in the similar systems.

The waste heat may not always be stable since the heat dissipation could change frequently. However, the temperature of components is maintained as relatively stable since the sophisticated electronics usually contain thermal management functionalities. Therefore, we carried out several investigations into fixed junction temperatures. Thermal resistance by the interface between the junction and the hot side of TE is assumed constant at $\psi_h$= 0.01[K/W]. The ambient temperature is fixed to $T_a$=35°C and the heat source temperature $T_s$ is set to 90, 100, 120, 150 and 200°C. Temperature ratio $T_a/T_s$ is in between 0.85 and 0.65. Three different scales are investigated as a) 30x30mm for a package, b) 3x3mm for a small chip, and c) 300x300μm for a hot spot.

Figs. 3-5 show the net power output in respect to the heat flux of the source device. For the larger case a), the harvesting levels are quite low while using air convection. Using water cooling, the power output curves are the same as air convection but heat flux increases continuously as heat flux increases. The pumping power needed for water cooling is more than four orders of magnitude smaller than air convection, based on Eq. (12), so that limitation is not observed until heat flux reached $10^7$ [W/m$^2$] order. Higher temperatures yield better performance, as Eq. (12) clearly suggests. From the study, if the water cooling is available, energy payback is practical in up to $10^7$ [W/m$^2$] order heat flux, and the higher $T_j$ provides practical energy payback. Similarly, air cooling is not a good solution for the waste heat recovery for electronic devices.

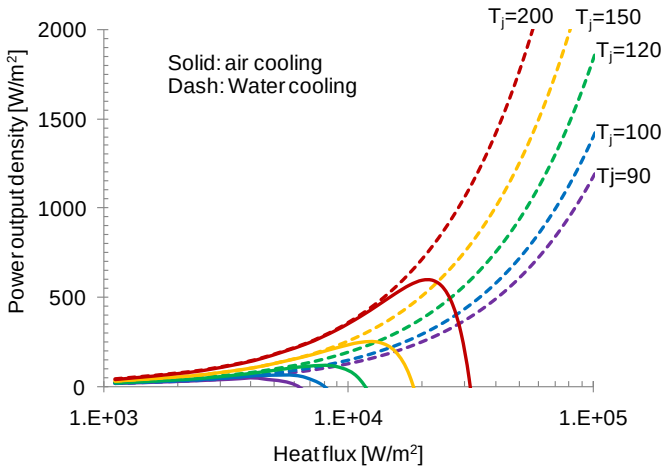


Figure 3. Net power output per unit area vs input heat flux. The device area is 30x30mm.

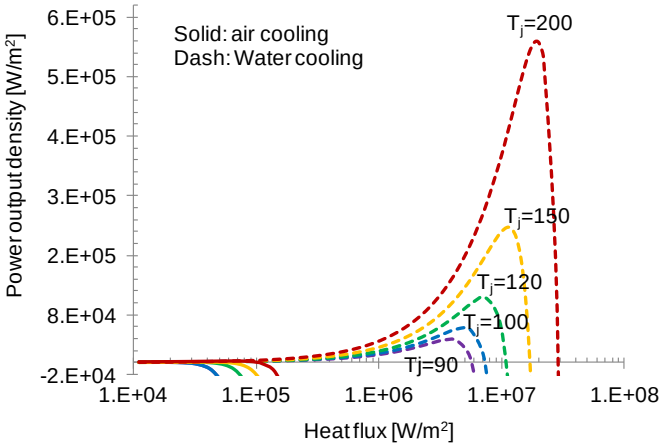


Figure 4. Net power output per unit area vs input heat flux. The device area is 3x3mm.

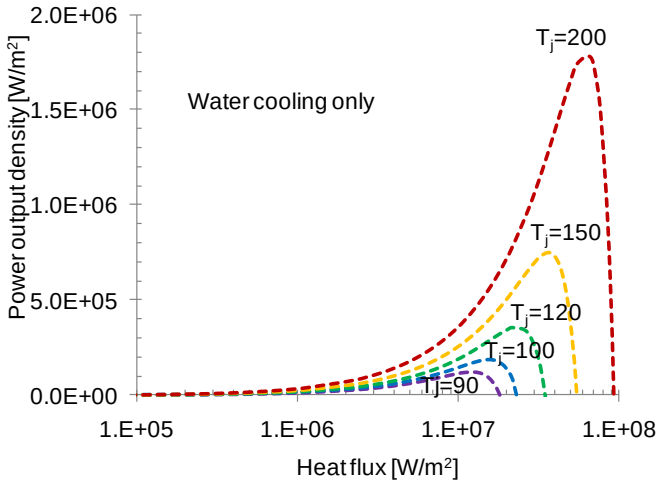


Figure 5. Net power output per unit area vs input heat flux. The device area is 300x300μm.


Copyright © 2011 by ASME

## COST IMPACT

Based on our previous study [10], the small fractional area ratio of the thermoelectric element in respect to the heat flow cross section area was found mass effective. This trend helps both cost savings and light weight considerations even for the ordinal thermoelectric materials with ZT=1. The results are very similar to the previous study so that we will give the typical numbers here. But obviously it is limited for water cooling solution. The TE material cost by different fractional area $F$=100%, 10%, and 1% are $7.8\text{x}10^3$, $2.4\text{x}10^2$, and 7.8 \$/m$^2$ respectively. The ZT is the same as above, the heat flux is $2\text{x}10^5$ W/m$^2$, the raw material price is 500\$/kg for $Bi_2Te_3$ thermoelectric element and 100\$/kg for AlN substrate.

## MAXIMUM POWER GENERATION

Before discussing the wide range analysis on entropy generation and the exergy of the waste heat recovery system, here we discuss the maximum power generation for latter comparison. We took the liberty to vary the external thermal resistance to cover any case of thermal management. Fig. 6 shows the power output and heat flow for different external thermal resistances ratios $\psi_c/\psi_h$ where the source temperature $T_s$ and ambient temperature $T_a$ is fixed.

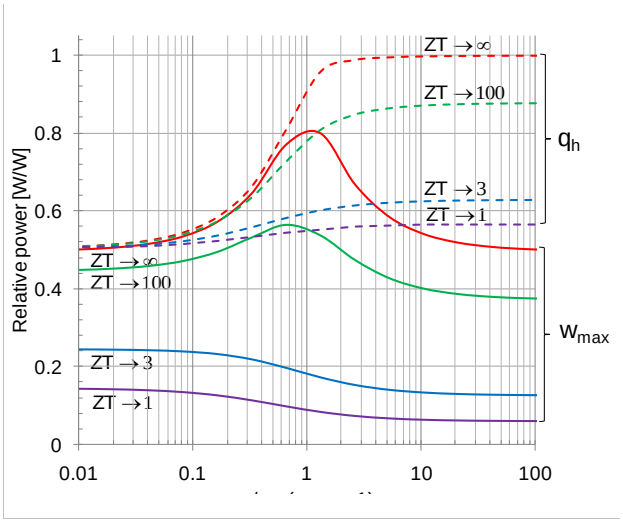


Figure 6. Normalized Power and heat by the maximum heat vs $\psi_c/\psi_h$ with varying ZT. Ta/Ts=0.01.

In the case of $\psi_c+\psi_h=1$, the maximum power output is observed at the smallest $\psi_c/\psi_h$ and the peak is found at off symmetric at around ZT of 5.1. It gradually converges to the symmetric as ZT values keep increasing.

## ENTROPY GENERATION IN POWER GENERATION

Entropy generation in a thermoelectric power generation system can be described as,

$$\dot{S}_{gen} = \frac{\partial S}{\partial t} + \left(\frac{q_h}{T_h} - \frac{q_h}{T_s}\right) + \left(\frac{q_c}{T_c} - \frac{q_h}{T_h}\right) + \left(\frac{q_c}{T_a} - \frac{q_c}{T_c}\right) > 0 \quad (24)$$

while power output $w = q_h - q_c$. The first right term of Eq. (24) is equal to zero considering the steady-state behavior of the model. By substituting heat flow $q_h$ and $q_c$ by definition of thermal resistances, the entropy generation becomes,

$$\dot{S}_{gen} = \frac{(T_c - T_a)}{\psi_c T_a} - \frac{(T_s - T_h)}{\psi_h T_s} \quad (25)$$

Figs. 7 and 8 show examples of entropy generation for a variety of the ZT value and the ratio of external thermal resistances for an extremely large temperature difference and a 300K difference to the room temperature respectively. The data shows optimal design cases. It is clear that the smaller thermal resistance ratio $\psi_c/\psi_h$ yields less entropy generation. It is explained by Fig. 5. The heat flow at optimum design is lower when $\psi_c/\psi_h$ is lower. This is essentially caused by the lower entropy generation.

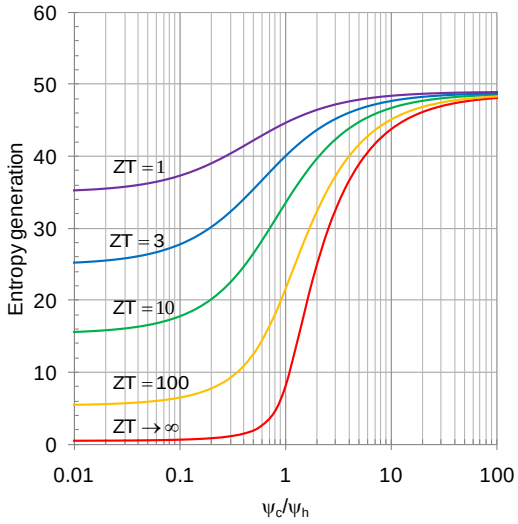


Figure 7. Entropy generation as a function of the ratio of external thermal resistances for different ZT values. $T_a/T_s$=0.01 for $T_a$=300K.


Copyright © 2011 by ASME

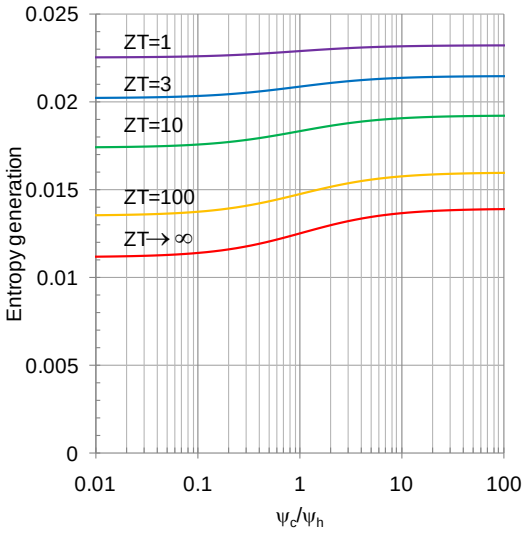


Figure 8. Entropy generation as a function of the ratio of external thermal resistances for different ZT values. $T_a/T_s$=0.8 for $T_a$=300K.

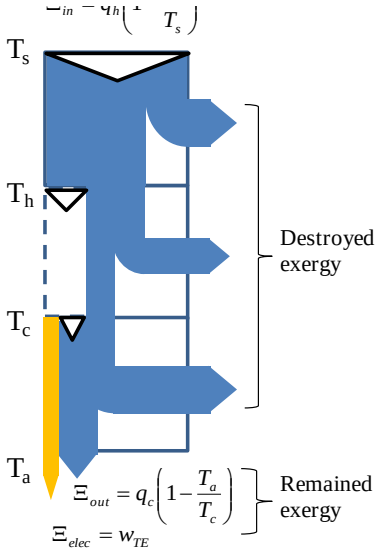


Figure 9. Exergy flow of a thermoelectric generation system.

It is obvious from Eq. (25) that the entropy generation linearly results to $1/\Sigma\psi$. The value of entropy generation changes by changing $\Sigma\psi$, but the above curves stay the same.

As Bejan [11] pointed out, the minimization of entropy generation is equivalent to the maximization of power output with symmetric dissipations. We reach the same conclusion only at infinite values of *ZT* (figure-of-merit), which occurs only in the ideal or reversible engine.

## EXERGY AT OPTIUM SYSTEM

By definition, exergy is the metric measure of the maximum possible work in a process. In this particular thermoelectric system, the exergy per unit area $\Xi$ [W/m$^2$] is found as the product of the heat flow per unit area in steady state and Carnot efficiency. The entire system can be expressed as shown in Fig. 9 where destroyed exergy exits to right and the delivered exergy exits down word (see [12]).

The exergy is destroyed at the three stages of the system including - $\psi_h$, $\psi_c$, and thermoelement. Thus, remained exergy is found as

$$\Xi = w + q_c\left(1-\frac{T_a}{T_c}\right) \tag{26}$$

where $w$ is the TE power output per unit area, and $q_c$ is the wasted heat per unit area flows in the cold side thermal path.

Fig. 10 shows an example of the exergy per unit area at the optimum design respect to ZT for different external thermal conditions. Electricity contribution of the exergy significantly increases by increasing ZT and gradually converges to a certain level. The electricity contribution is almost identical for any asymmetric thermal resistance systems. For a smaller $\psi_c$, remained exergy, which is unconverted heat, is observed to be the smallest and consequently the system generates the highest quality of energy output. As $\psi_c/\psi_h$ increases the remained exergy increases. It is caused by the larger heat contribution of the cold side heat sink in the downstream of the system. This large amount of heat contribution for large $\psi_c/\psi_h$ (>1) suggests potential opportunity of co-generation.


Copyright © 2011 by ASME

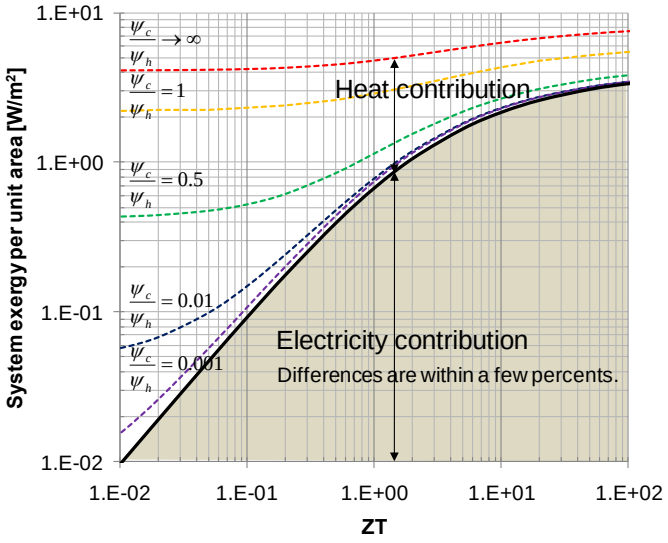


Figure 10. The normalized exergy as a function of the ratio of external thermal resistances and for different ZT values. $T_a/T_s$=0.8 for $T_a$=300K.

## CONCLUSIONS

We discussed the energy payback of the thermoelectric waste heat recovery from the electronics. The generic analytic model of thermoelectric power generation systems was introduced. The pumping power was found to introduce a thermoelectric generator into the middle of the thermal management system. Minimizing the pumping power led to an optimum heat sink design, and the model was integrated into the whole analysis. The power output, depending on the heat flux, was found for three typical heat source sizes. These represent an IC package, a small chip, and a hot spot on a chip. Water cooling was found effective for the entire range of the practical heat flux if the thermal conductivity was unlimited for the heat sink material. The power output for a smaller junction temperature was not only low, but it significantly limited the possibility of using air cooling. The cost impact assuming the typical material price was analyzed. The smaller fractional area showed a dramatically lower cost for the thermoelectric material, rather the heat sink material cost was found to be the dominant consideration. This suggests the impact of the cost for waste heat recovery can be reduced if the parasitic challenges such as heat leak and contact resistance are solved. Entropy generation was investigated for the maximum power output based on the model. The results indicated that minimum entropy generation occurs in symmetric thermal dissipation only while the figure-of-merit goes to infinity. We also carried out exergy analysis on the maximum power output model. Larger cold side thermal resistance shows the larger heat contribution of remained exergy which suggest the opportunity of co-generation.

## ACKNOWLEDGMENTS

This work was supported by Center for Energy Efficient Materials funded by the Office of Basic Energy Sciences of the US Department of Energy.

## REFERENCES

[1] H. A. Sodano, D. J. Inman, G. Park, “A Review of Power Harvesting from Vibration Using Piezoelectric Materials”, The Shock and Vibration Digest, Vol. 36, Issue 3, pp 197-205, 2004.
[2] A.J. Jansen, A.L.N. Stevels, “Human power, a sustainable option for electronics”, Proceedings of the 1999 IEEE International Symposium on Electronics and the Environment, pp215 – 218, 1999.
[3] G. Dennler and N. S. Sariciftci, “Flexible Conjugated Polymer-Based Plastic Solar Cells: From Basics to Applications”, Proceedings of the IEEE, Viol. 93, No. 8, pp1429-1439, 2005.
[4] K. Yazawa, G. Solbrekken and A. Bar-Cohen, “Thermoelectric-powered convective cooling of microprocessors”, IEEE Transaction on Advanced Packaging Technologies, Vol. 28, Issue 2, pp231 – 239, 2005.
[5] F. L. Curzon and B. Ahlborn,” Efficiency of a Carnot engine at maximum power output”, American Journal of Physics. Volume 43, Issue 1, pp. 22, 1975.
[6] K. Yazawa and A. Shakouri, “Asymmetric Thermodynamic Behavior of Thermoelectric Power Generation Systems”, Phys. Rev. Lett. – in review
[7] M. Esposito, R. Kawai, K. Lindenberg and C. Van den Broeck, “Efficiency at Maximum Power of Low-Dissipation Carnot Engines”, Physical Review Letters. Vol. 105, 150603, 2010.
[8] K. Yazawa and A. Shakouri, “Energy Payback Optimization of Thermoelectric Power Generator Systems”, Proceedings of ASME IMECE2010, IMECE2010-37957, 2010.
[9] A. Bejan, Advanced Engineering Thermodynamics, Wiley, 1988
[10] G. L. Solbrekken, K. Yazawa and A. Bar-Cohen, Heat Driven Cooling of Portable Electronics Using Thermoelectric Technology, IEEE Transaction on Advanced Packaging, Vol.31, No.2, pp.497-437, 2008.
[11] K.K. Shah and M.S. Bhatti, “Laminar Convection Heat Transfer in Ducts”, Handbook of Single Phase Convective Heat Transfer, 1987.
[12] A. Bejan, Entropy Generation Minimization, CRC Press, pp249-252, 1948


Copyright © 2011 by ASME